

## Article

# Energy and Exergy Analysis of the Air Source Transcritical CO<sub>2</sub> Heat Pump Water Heater Using CO<sub>2</sub>-Based Mixture as Working Fluid

Yikai Wang <sup>1</sup>, Yifan He <sup>1</sup>, Yulong Song <sup>1,\*</sup>, Xiang Yin <sup>1</sup>, Feng Cao <sup>1,\*</sup> and Xiaolin Wang <sup>2</sup> 

<sup>1</sup> School of Energy and Power Engineering, Xi'an Jiaotong University, Xi'an 710049, China; zdxrdwyk@163.com (Y.W.); heyifan9889@163.com (Y.H.); xiangyin@mail.xjtu.edu.cn (X.Y.)

<sup>2</sup> School of Engineering, University of Tasmania, Hobart, TAS 7001, Australia; xiaolin.wang@utas.edu.au

\* Correspondence: yulong.song@mail.xjtu.edu.cn (Y.S.); fcao@mail.xjtu.edu.cn (F.C.); Tel.: +86-29-8266-3583 (Y.S.); +86-29-8266-3583 (F.C.)

**Abstract:** Given the large demand nowadays for domestic hot water, and its impact on modern building energy consumption, air source transcritical CO<sub>2</sub> heat pumps have been extensively adopted for hot water production. Since their system efficiency is limited by significant irreversibility, a CO<sub>2</sub>-based mixture could offer a promising drop-in technology to overcome this deficiency without increasing system complexity. Although many CO<sub>2</sub> blends have been studied in previously published literature, little has been presented about the CO<sub>2</sub>/R32 mixture. Therefore, a proposed mixture for use in transcritical CO<sub>2</sub> heat pumps was analyzed using energy and exergy analysis. Results showed that the coefficient of performance and exergy efficiency variation displayed an “M” shape trend, and the optimal CO<sub>2</sub>/R32 mixture concentration was determined as 0.9/0.1 with regard to flammability and efficiency. The irreversibility of the throttling valve was reduced from 0.031 to 0.009 kW·kW<sup>-1</sup> and the total irreversibility reduction was more notable with ambient temperature variation. A case study was also conducted to examine domestic hot water demand during the year. Pure CO<sub>2</sub> and the proposed CO<sub>2</sub> blend were compared with regard to annual performance factor and annual exergy efficiency, and the findings could provide guidance for practical applications in the future.

**Keywords:** transcritical CO<sub>2</sub> heat pump; energy analysis; exergy analysis; CO<sub>2</sub>-based mixture; ambient temperature; case study



**Citation:** Wang, Y.; He, Y.; Song, Y.; Yin, X.; Cao, F.; Wang, X. Energy and Exergy Analysis of the Air Source Transcritical CO<sub>2</sub> Heat Pump Water Heater Using CO<sub>2</sub>-Based Mixture as Working Fluid. *Energies* **2021**, *14*, 4470. <https://doi.org/10.3390/en14154470>

Academic Editor: Patrick Phelan

Received: 30 June 2021

Accepted: 21 July 2021

Published: 23 July 2021

**Publisher's Note:** MDPI stays neutral with regard to jurisdictional claims in published maps and institutional affiliations.



**Copyright:** © 2021 by the authors. Licensee MDPI, Basel, Switzerland. This article is an open access article distributed under the terms and conditions of the Creative Commons Attribution (CC BY) license (<https://creativecommons.org/licenses/by/4.0/>).

## 1. Introduction

Nowadays, with rapid urban construction and development, building energy consumption is increasing equally rapidly in China [1]. Domestic hot water (DHW) requirements dominate and account for 40–50% of energy consumption [2]. As an environmentally friendly and efficient solution, the air source heat pump (ASHP) is advocated as an alternative method to conventional solutions [3]. Furthermore, following publication of the Montreal Protocol and the EU F-Gas Regulation, the use of traditional hydrofluorocarbons is gradually being phased out. Given its superior non-flammable and non-toxic properties, the use of natural CO<sub>2</sub> as a safe refrigerant has attracted the attention of researchers [4]. Furthermore, its temperature glide matches well with the water temperature lift. Therefore, an air source transcritical CO<sub>2</sub> heat pump (TCHP) water heater should be the preferred choice for DHW.

However, for the basic cycle, the large pressure difference and huge irreversibility caused by the throttling value limit and even deteriorate the efficiency of the system. To overcome this weakness, many methods have been proposed in the published literature: internal heat exchangers (IHX) [5], ejectors [6], expanders [7], subcooling [8], flash gas bypass [9], parallel compression [10], two-stage compression [11], evaporative cooling [12], and CO<sub>2</sub>-based mixtures. With the IHX, the coefficient of performance (COP) can be

optimized by controlling the gas cooler pressure [5]. Under fixed ejector geometries, Taleghani et al. [6] concluded that the COP can be improved by about 17% under the same operating conditions. In an identical experiment configuration, Yang et al. [7] substituted an expander for the throttling valve, and the system exergy efficiency was enhanced by 33%. With direct dedicated mechanical subcooling, the maximum COP was found to be obtained at the optimal subcooling degree [8]. By adding flash gas bypass into the basic cycle, Elbel and Hrnjak [9] pointed out that the cooling capacity could be increased by up to 9%. Although limited by ineffective separation, the COP was still increased by 10% with the parallel compression cycle proposed by Chesi et al. [10]. With the proposed double-compression flash intercooling system, the basic cycle efficiency could be increased by 23.18% [11]. De Antonellis et al. [12] theoretically and experimentally investigated the indirect evaporative cooling system, and the effect of different factors was also evaluated.

The above technologies will, nevertheless, increase system complexity and require additional equipment [13]. The system's initial capital cost will consequently be increased, leading to a longer payback period. Therefore, a CO<sub>2</sub>-based refrigerant mixture could offer a promising drop-in technology to consider. [14].

For CO<sub>2</sub>-based mixtures, there are many refrigerants with low global warming potential (GWP) that have attracted researchers' attention. Currently, CO<sub>2</sub>/propane blends are widely used in vapor compression refrigeration and heat pump fields [15]. Niu and Zhang [16] studied the R744/propane mixture to replace the refrigerant R13, and the proposed mixture was a promising refrigerant if the evaporator temperature was above 201 K. Zhang et al. [17] developed a system mode to study optimum concentration, and suggested that the optimum CO<sub>2</sub> fraction should be higher than 78%. Based on their experimental and simulation study, Ju et al. [18] analyzed the effect of the R744/propane mixture concentration, and the optimum concentration was found to be 12%/88%. Furthermore, using the identified optimal concentration, Ju et al. [19] experimentally compared the R744/propane mixture with pure R22 for domestic hot water supply, and the results showed that the system COPs were 4.98–11.00% higher under a variety of working conditions.

Attention has also been paid to CO<sub>2</sub>/R41 blends in previously published literature. Wang et al. [20] used thermodynamic analysis to compare pure CO<sub>2</sub> refrigerant with CO<sub>2</sub>/R41 blends. This mixture was proved to be an excellent substitute because of the lower discharge pressure and higher COP. Similarly, by comparing various refrigerants on the basis of thermodynamic analysis, Dai et al. [21] also indicated that CO<sub>2</sub>/R41 blends were proved to be suitable candidates for DHW. With the CO<sub>2</sub>/R41 blends charged into automobile systems, the energy efficiency was improved by 14.5% in heating mode and 25.7% in cooling mode [22].

However, the mixture of environmental refrigerant R32 with CO<sub>2</sub> has seldom been studied in previous literature, nor has there been any study of optimum concentration. With regard to flammability and applicability, although the higher GWP is obtained by R32, it is superior to R290 to some extent [23]. The exergy analysis, in which the exergy efficiency and irreversibility can be studied in detail, can provide guidance for further system improvement. As a result, a proposed CO<sub>2</sub>/R32 mixture refrigerant has been theoretically investigated in this paper. The mass fraction effect and comparison with the pure refrigerant have also been analyzed based on energy and exergy analysis.

## 2. System Modeling

### 2.1. System Description

The schematic diagram of the air source transcritical CO<sub>2</sub> heat pump water heater is shown in Figure 1. The system is composed of the compressor, gas cooler, electronic expansion valve (EEV), and evaporator. The system cycle is described as follows: (1) 1–2: non-isentropic compression; (2) 2–3: releasing heat to the water; (3) 3–4: isenthalpic throttling in the EEV; (4) 4–1: absorbing heat from the air.

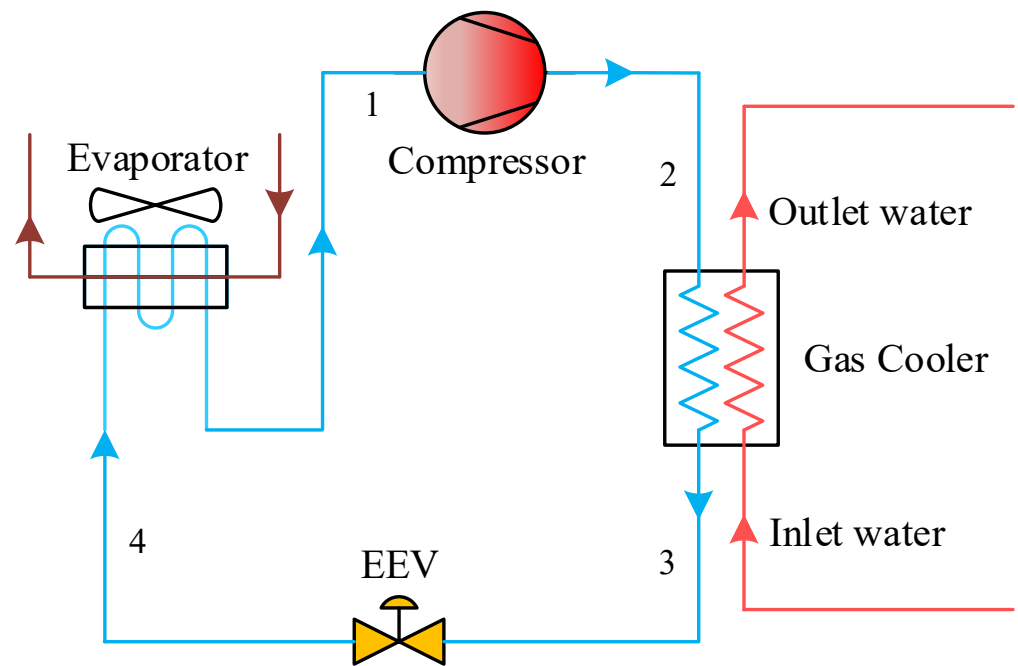


**Figure 1.** Schematic diagram of the air source transcritical CO<sub>2</sub> heat pump water heater.

The property of R32 is summarized in Table 1.

**Table 1.** The specific properties of environmental refrigerant R32.

Fluid	Molecular Mass	Boiling Temperature	Critical Temperature	Critical Pressure	ODP	GWP	ASHRAE 34 Safety Group
R32	52.02	−51.7 °C	78.1 °C	5.78 MPa	0	675	A2

Data from Refprop 9.1 [24].

## 2.2. System Assumptions

The assumptions adopted in the thermodynamic analysis in this paper are presented as follows:

1. The system operates under steady conditions.
2. Heat loss and pressure drop during the heat transfer process is ignored.
3. The influence of gravity and kinetic energy is ignored.
4. The refrigerant is saturated at the evaporator outlet.

## 2.3. Energy Analysis Method

The system's energetic performance was evaluated based on the presented equations, and the CO<sub>2</sub>-based mixture properties were gained from Refprop 9.1 [24]. The inlet/outlet water temperatures were assumed and fixed at 15 and 55 °C based on the Chinese testing standard [25]. The CO<sub>2</sub>-based mixture state was calculated with the pinch point temperature difference at the gas cooler and evaporator as listed in Table 2.

**Table 2.** The assumptions used in the energy analysis.

Symbol	Meaning	Unit	Value
$\eta_m$	Compressor mechanical efficiency	-	0.9
$\eta_e$	Compressor electrical efficiency	-	0.9
$\eta_{is}$	Compressor isentropic efficiency	-	0.8
$\dot{m}_r$	Refrigerant mass flow rate	kg·s <sup>-1</sup>	1
$\Delta T_a$	Temperature difference between the air inlet and outlet	°C	5
$\Delta T_{GC,pinch}$	Pinch point temperature difference in the gas cooler	°C	5
$\Delta T_{Evap,pinch}$	Pinch point temperature difference in the evaporator	°C	5

Data from the reference [21].

Compressor:

$$W_{Comp} = \dot{m}_r(h_2 - h_1) / (\eta_m \eta_e) \quad (1)$$

$$\eta_{is} = (h_{2s} - h_1) / (h_2 - h_1) \quad (2)$$

Gas cooler:

$$Q_h = \dot{m}_r(h_2 - h_3) \quad (3)$$

$$m_w = \dot{m}_r(h_2 - h_3) / (h_{w,out} - h_{w,in}) \quad (4)$$

Electronic expansion valve:

$$h_4 = h_3 \quad (5)$$

Evaporator:

$$Q_c = \dot{m}_r(h_1 - h_4) \quad (6)$$

$$m_a = \dot{m}_r(h_1 - h_4) / (h_{a,in} - h_{a,out}) \quad (7)$$

For the total system:

$$COP = Q_h / W_{Comp} \quad (8)$$

#### 2.4. Exergy Analysis Method

The system's exergetic performance was evaluated based on the presented equations, and  $T_0$  refers to the dead state. In this section, the heat pump system and the external environment were considered as a whole, and the exergy destruction due to irreversible heat transfer in the presented equations includes the exergy destruction between the refrigerant and the component, and the exergy destruction between the ambient fluid and the component.

Compressor:

$$I_{Comp} = \dot{m}_r T_0 (s_2 - s_1) \quad (9)$$

Gas cooler:

$$I_{GC} = \dot{m}_r T_0 (s_3 - s_2) - m_w T_0 (s_{w,i} - s_{w,o}) \quad (10)$$

Electronic expansion valve:

$$I_{EEV} = \dot{m}_r T_0 (s_4 - s_3) \quad (11)$$

Evaporator:

$$I_{Evap} = m_a T_0 (s_{a,o} - s_{a,i}) - \dot{m}_r T_0 (s_4 - s_1) \quad (12)$$

Irreversibility per unit heating capacity of each component:

$$ir = I_k / Q_h \quad (13)$$

where,  $I_k$  represents the irreversibility of each component.

System total irreversibility:

$$I_{Tot} = I_{Comp} + I_{GC} + I_{TV} + I_{Evap} \quad (14)$$

System exergy efficiency:

$$\eta = 1 - I_{Tot}/W_{Comp} \quad (15)$$

### 3. Results and Discussion

#### 3.1. Effect of CO<sub>2</sub>-Based Mixture Fraction

The GWP calculation method for the mixture refrigerant is as follows [20]:

$$GWP_{Mix} = GWP_{CO_2} \cdot \omega_{CO_2} + GWP_{R32} \cdot \omega_{R32} \quad (16)$$

The GWP of the CO<sub>2</sub>/R32 mixture is shown in Figure 2. As can be seen, with an increased R32 mass fraction, the GWP of the mixture increases linearly. According to the calculated GWP result of the CO<sub>2</sub>/R32 mixture and the GWP classification [26], if the mass fraction of R32 is 0.1, the mixture is a “very low GWP” refrigerant. If the mass fraction of R32 is within 0.2–0.4, the mixture is a “low GWP” refrigerant, and otherwise a “medium GWP” refrigerant. Excessive temperature glide, as indicated in the literature [27], will lead to a high concentration shift, and even mixture fractionation. Therefore, the temperature glide of the CO<sub>2</sub>-based mixture is first analyzed. With the mass fraction of organic fluid increasing from 0 to 1, with an interval of 0.1, the temperature glide of the CO<sub>2</sub>-based mixture is depicted in Figure 2 at the bubble point temperature of 0 °C. Clearly the temperature glide is first increased and then gradually decreased with the increased R32 mass fraction, leading to the existence of a maximum temperature glide. Considering the different boiling temperatures of the refrigerants CO<sub>2</sub> and R32, the temperature glide is correlated with this difference and the maximum temperature glide of 14.20 °C is obtained with the CO<sub>2</sub>/R32 mass fraction of 0.4/0.6. Consequently, the temperature glide variation range of the CO<sub>2</sub>/R32 mixture is acceptable.

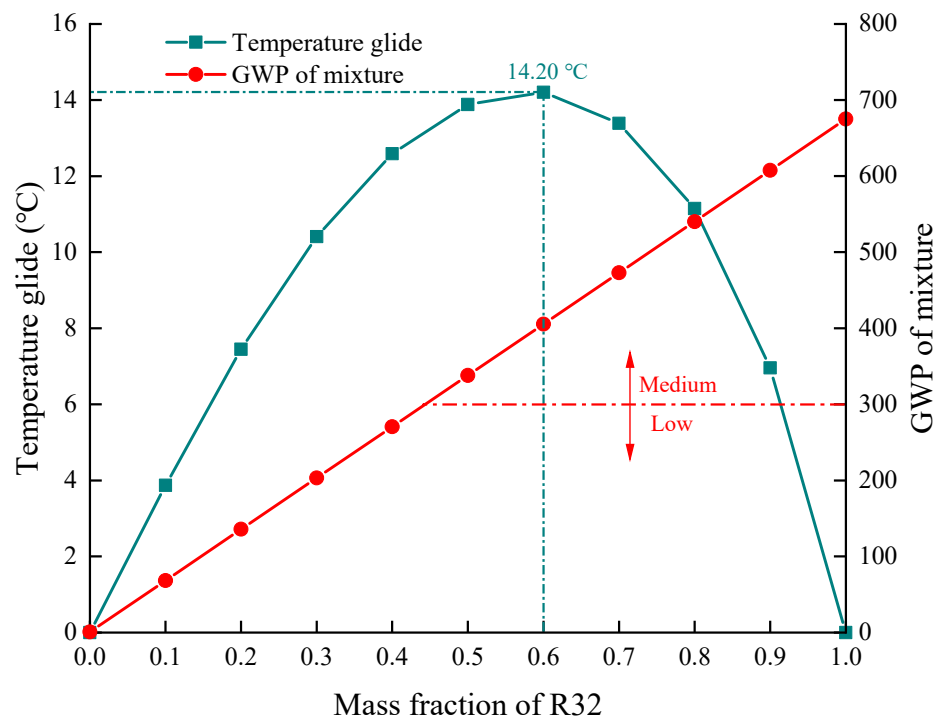
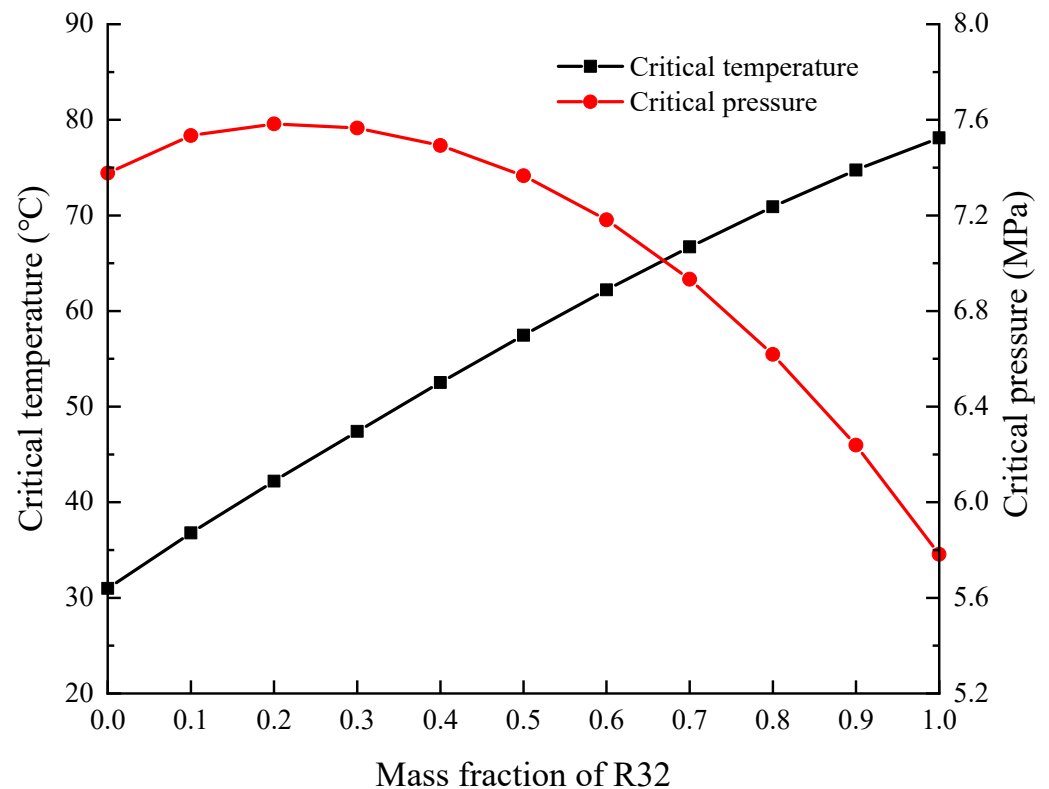


Figure 2. Temperature glide and GWP of the CO<sub>2</sub>-based mixture.

The critical temperature and critical pressure are shown in Figure 3. For the critical pressure, the variation tendency is the same as that of the temperature glide, also increasing first and then decreasing with the enlarged R32 mass fraction. For the pure CO<sub>2</sub> and R32, the critical pressure is 7.38 MPa and 5.78 MPa, respectively. At the CO<sub>2</sub>/R32 mass fraction of 0.8/0.2, the maximum critical pressure of 7.58 MPa is obtained. The critical temperature is always increasing with the larger R32 mass fraction because of the higher R32 critical temperature. However, with regard to system safety and flammability of the organic fluid, the mass fraction of the natural refrigerant CO<sub>2</sub> is suggested to be higher than 0.3 [28].



**Figure 3.** Critical temperature and critical pressure of the CO<sub>2</sub>-based mixture.

In order to compare the effect of the mass fraction of R32 on the system's maximum COP, the calculated COP results at the optimal discharge pressure, at an ambient temperature of 15 °C, are depicted in Figure 4. Interestingly, the COP variation is not increased or decreased in a straight upward or downward trend. Instead, the variation shows a trend similar to that of the letter "M". When compared to the COP for a system charged with the pure CO<sub>2</sub> refrigerant, the system COP is 0.30–4.25% higher if the mass fraction of R32 is within 0.1–0.3 and 0.41–6.07% higher if it is within 0.7–0.9. With an R32 mass fraction of 0.4–0.6, the system COP is much lower, and the minimum COP is achieved with an R32 mass fraction of 0.5. Therefore, this concentration cannot be adopted due to the lower energy efficiency. Furthermore, although the maximum COP is obtained by a CO<sub>2</sub>/R32 mixture mass fraction of 0.1/0.9, this concentration is also not recommended due to the higher flammability.

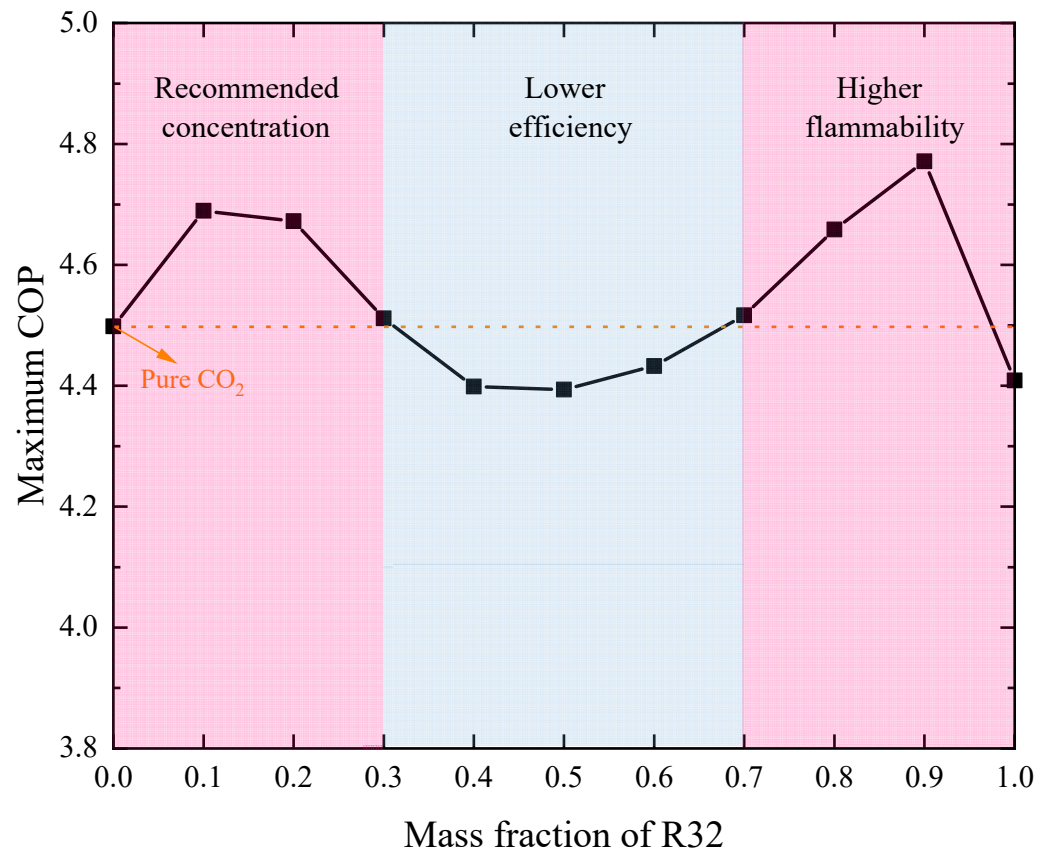


Figure 4. The maximum COP across the R32 mass fraction range.

In addition to improving the system heating performance, a further benefit of using the mixed refrigerant is a reduction in the system discharge pressure. As shown in Figure 5, the optimal discharge pressure gradually declines with increased R32 mass fraction, and this pressure reduction is more significant the higher the R32 mass fraction. Regardless of the system COP, the highest optimal discharge pressure is 9.25 MPa presented by pure CO<sub>2</sub> and the lowest is 3.3 MPa achieved by pure R32. Therefore, adopting this refrigerant mixture will certainly ensure the system's operational safety. Furthermore, with the critical pressure presented in Figure 3, the transcritical CO<sub>2</sub> heat system will be shifted to the subcritical cycle if the R32 mass fraction is higher than 0.2.

For the exergetic performance, the irreversibility per unit heating capacity of each component at an ambient temperature of 15 °C is illustrated in Figure 6. For the basic CO<sub>2</sub> cycle, the largest irreversibility is for the throttle valve, due to the higher pressure difference. With the increased R32 mass fraction, as expected, the irreversibility of the throttle valve can be significantly reduced from 0.031 to 0.009 kW·kW<sup>-1</sup>, with a corresponding proportion of 28.38% to 8.00%. This phenomenon can be explained with the pressure reduction as depicted in Figure 5, since the lower pressure difference is beneficial for reducing the irreversible loss of the throttle valve. The irreversibility of the compressor is the second largest among the studied equipment and also gradually declines for the same reason. The largest total irreversibility is 0.114 kW·kW<sup>-1</sup> with an R32 mass fraction of 0.5, which is 3.95% higher than that of the pure CO<sub>2</sub> refrigerant. The lowest total irreversibility is 0.099 kW·kW<sup>-1</sup> with a CO<sub>2</sub> mass fraction of 0.1, meaning that the maximum exergy efficiency can be expected. Furthermore, the total irreversibility shows an opposite trend to the COP curve, meaning that the higher exergy efficiency can be expected at lower total irreversibility.

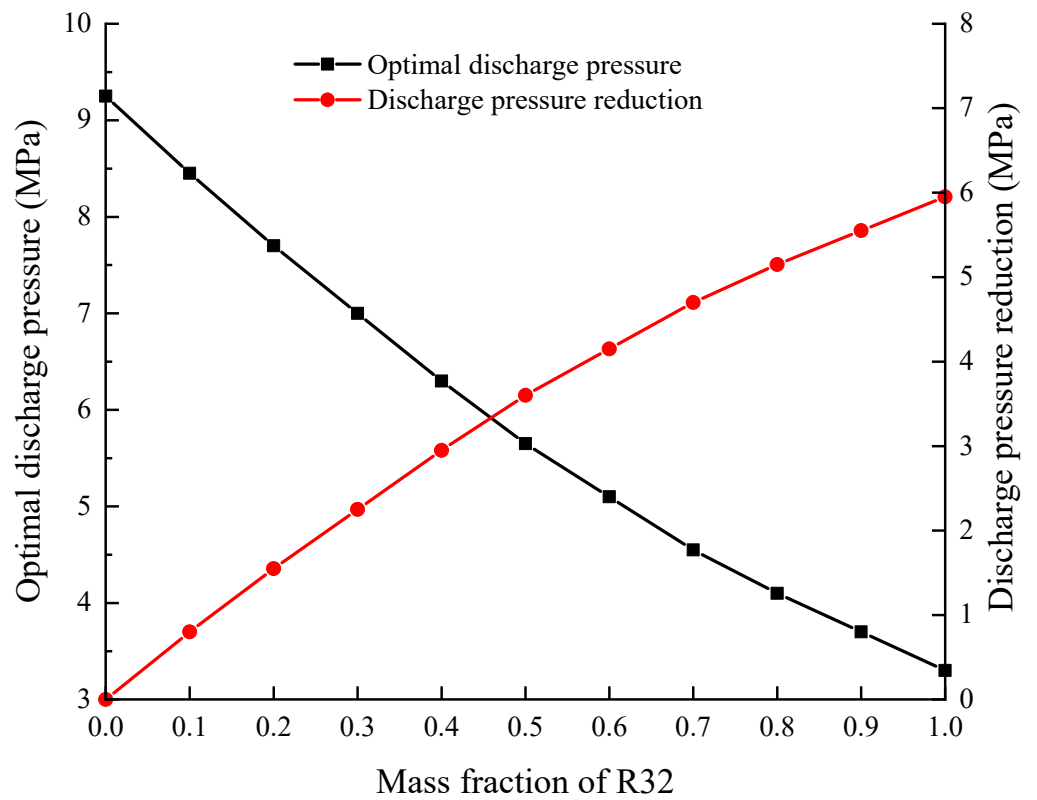


Figure 5. Optimal discharge pressure and pressure reduction across the R32 mass fraction range.

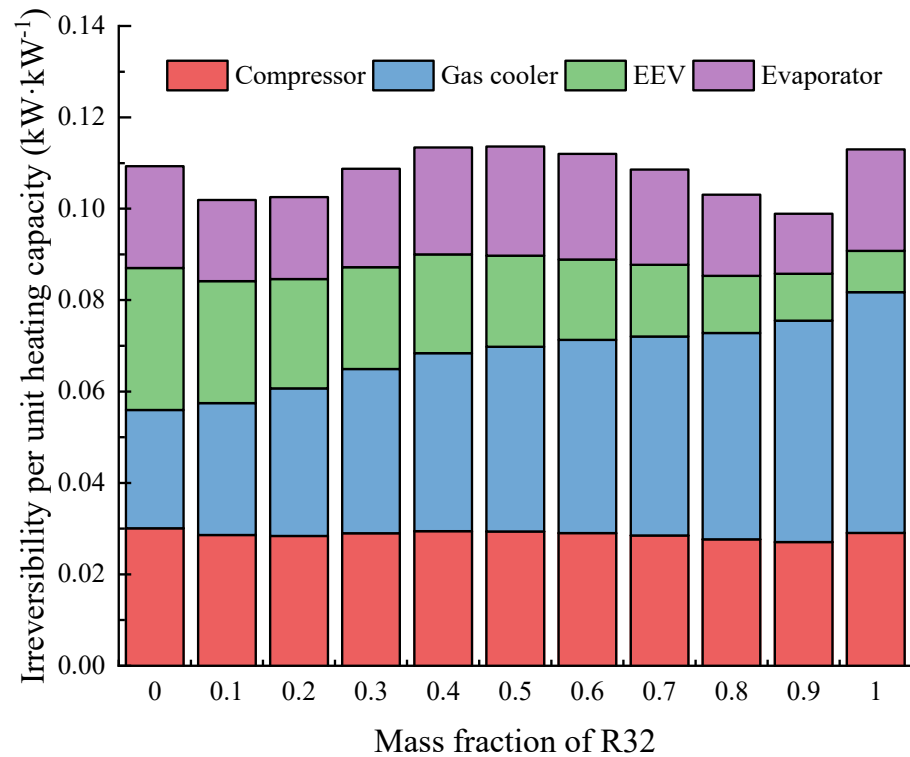
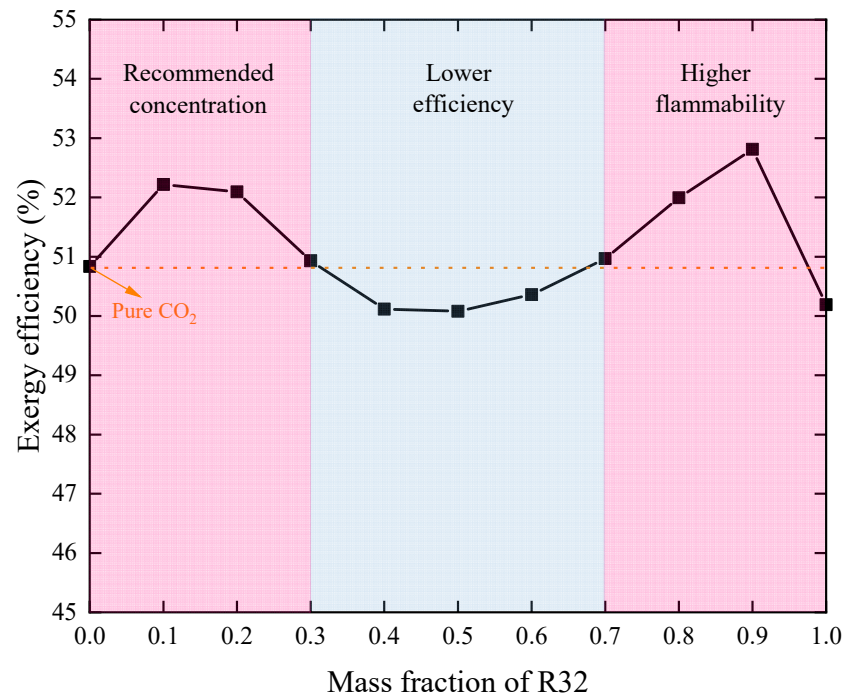


Figure 6. The irreversibility per unit heating capacity across the R32 mass fraction range.

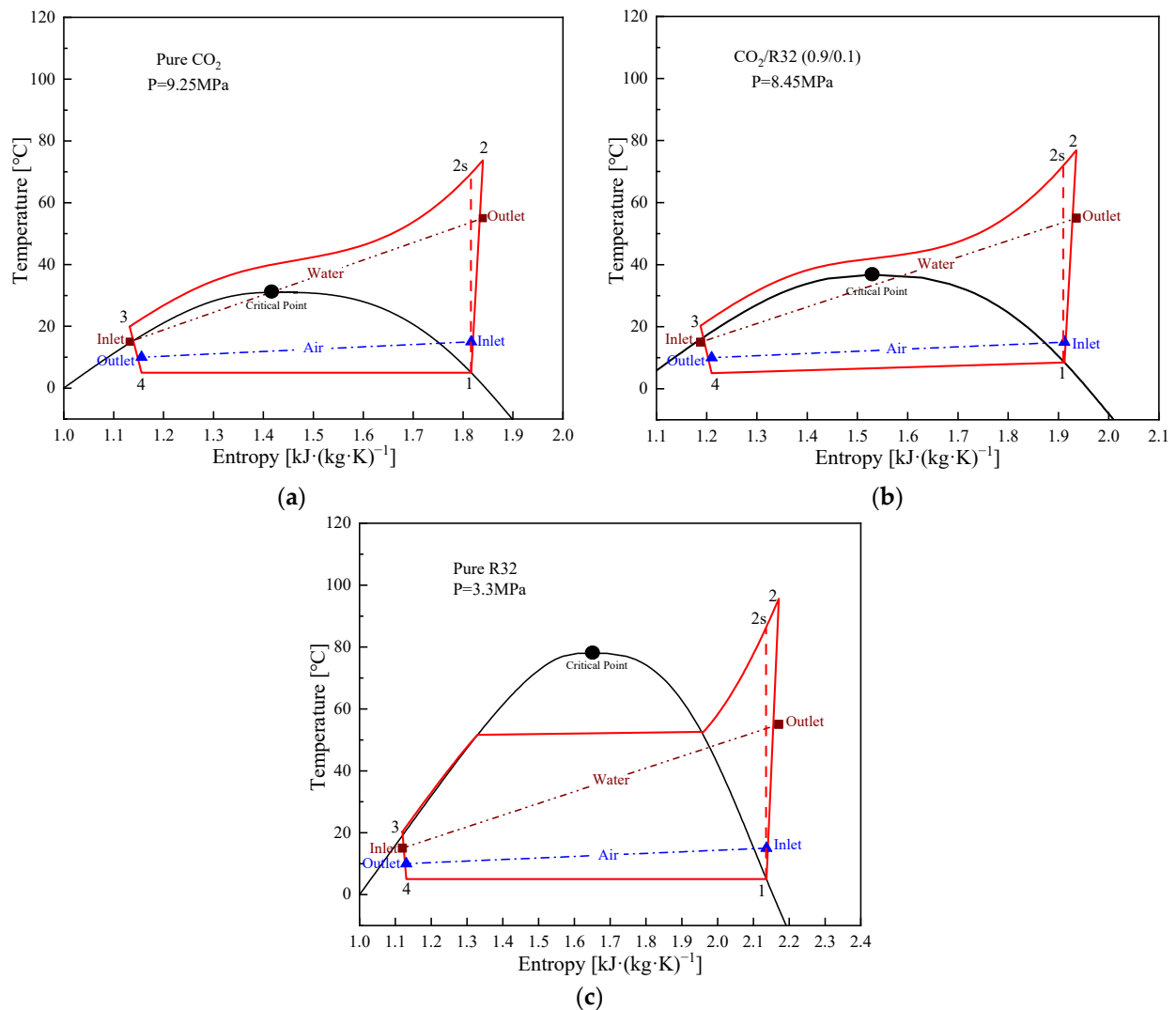
The exergy efficiency is an important factor that reflects the system’s optimal thermodynamic functioning. As depicted in Figure 7, the curve of the exergy efficiency at an ambient temperature of 15 °C also shows an “M” shape variation trend in relation to the

mass fraction of R32. At the R32 mass fraction corresponding to the maximum or minimum system COP, the maximum or minimum exergy efficiency is also obtained. Specifically, the maximum exergy efficiency is 52.81%, which is 3.89% greater than that of pure CO<sub>2</sub> refrigerant. Similarly, the lower exergy efficiency is achieved with an R32 mass fraction ranging from 0.4 to 0.6, which is 0.93–1.49% lower than that of a pure CO<sub>2</sub> cycle.



**Figure 7.** The exergy efficiency with the range of R32 mass fractions.

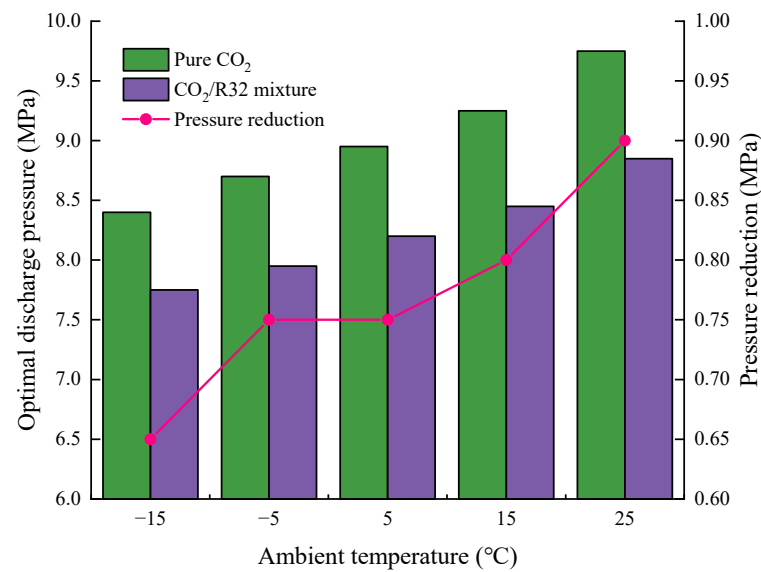
Therefore, based on the results discussed above, an R32 mass fraction of 0.1 to 0.3 is recommended, and the optimal mass fraction of the CO<sub>2</sub>/R32 mixture is 0.9/0.1. A comparison of the temperature-entropy diagram at the optimal system COP and discharge pressure is presented in Figure 8. Figure 8a,b show the transcritical cycles for pure CO<sub>2</sub> and CO<sub>2</sub>/R32 mixture refrigerants, and Figure 8c shows the subcritical cycle with pure R32. Since the temperature difference of the flowing water and ambient air are constant for the three cycles, a better thermal match will certainly result in a better COP. It is notable that the compressor discharge temperature is significantly increased from Figure 8a–c. This indicates that although the compressor discharge pressure can be reduced with R32, the greater mass fraction will lead to a deterioration in system safety, especially at lower ambient temperatures.



**Figure 8.** Temperature-entropy diagrams of the system cycle with (a) pure CO<sub>2</sub> refrigerant; (b) CO<sub>2</sub>/R32 mixture refrigerant; (c) pure R32 refrigerant.

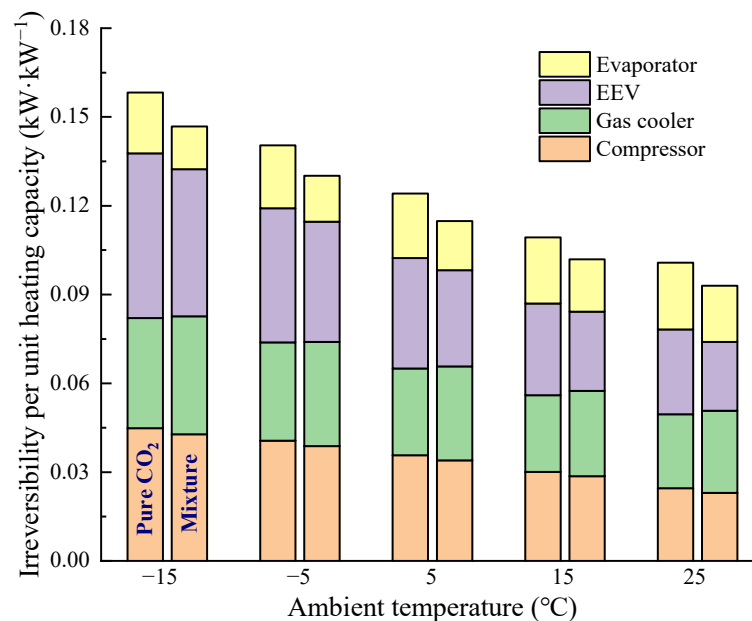
### 3.2. Effect of Ambient Temperature

Based on the identified optimal mass fraction of the CO<sub>2</sub>/R32 mixture, the effect of ambient temperature on pure CO<sub>2</sub> and CO<sub>2</sub>/R32 mixture refrigerants is further discussed in this section. The optimal discharge pressure of each cycle with respect to the ambient temperature of  $-15$  to  $25$  °C is shown in Figure 9. It is evident that, compared with the pure CO<sub>2</sub> cycle, system optimal pressure is always lower in the CO<sub>2</sub>/R32 cycle. The pressure reduction is increased from 0.65 MPa at the ambient temperature of  $-15$  °C to 0.9 MPa at  $25$  °C. Therefore, the pressure reduction is closely related to the external ambient temperature, and the proposed CO<sub>2</sub>/R32 mixture refrigerant is recommended to be adopted for cold climate working conditions.



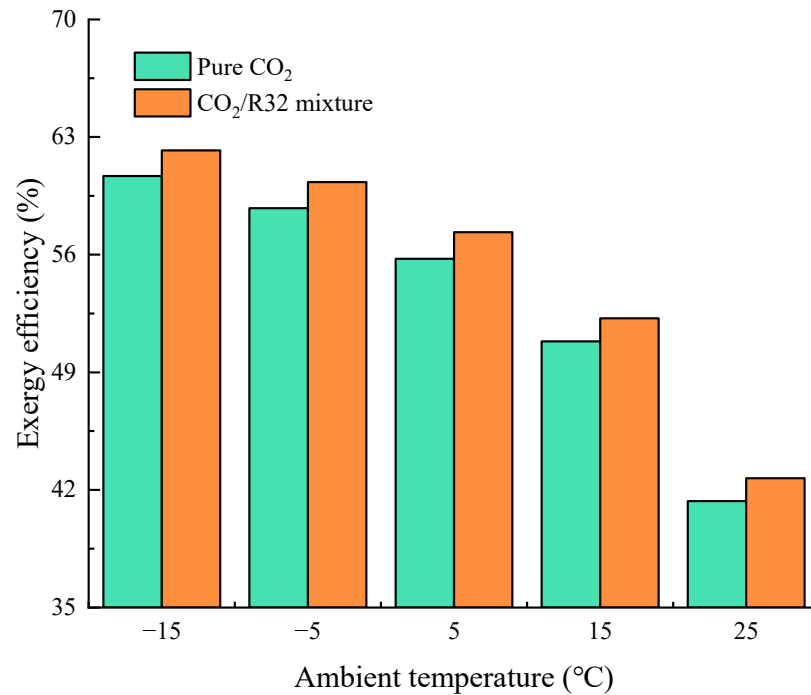
**Figure 9.** Comparison of the optimal discharge pressure with pure CO<sub>2</sub> and CO<sub>2</sub>/R32 mixture refrigerants at different ambient temperatures.

Figure 10 illustrates the results of the irreversibility per unit heating capacity of pure CO<sub>2</sub> and CO<sub>2</sub>/R32 mixture cycles at different ambient temperatures. The largest and smallest total irreversibility is 0.158 and 0.09 kW·kW<sup>-1</sup> at the ambient temperature of -15 °C and 25 °C, respectively. Regardless of the ambient temperature variation, the total irreversibility reduction is closely related to the irreversibility reduction of the throttling valve, and this reduction is varied from 6.77% to 7.76%. For each cycle, the irreversibility proportion of the EEV is reduced from 35.16% to 28.43% of the pure CO<sub>2</sub> cycle and from 33.83% to 25.02% of the CO<sub>2</sub>/R32 mixture cycle when the ambient temperature is increased from -15 °C to 25 °C. This also proves that the significant throttling irreversibility is lowered with the proposed CO<sub>2</sub>/R32 mixture refrigerant.



**Figure 10.** Comparison of the irreversibility per unit heating capacity with the pure CO<sub>2</sub> and determined CO<sub>2</sub>/R32 mixture under the varied ambient temperature.

Figure 11 compares the exergy efficiency with pure CO<sub>2</sub> and with CO<sub>2</sub>/R32 mixture refrigerants at different ambient temperatures. As can be seen, the exergy efficiency is always higher with the pure CO<sub>2</sub> cycle, and this enhancement is ranged from 1.36% to 1.58% in relation to the ambient temperature range of −15 to 25 °C. As shown in Figure 10, the irreversibility proportion of the EEV is much higher at lower ambient temperature, and the proposed CO<sub>2</sub>/R32 mixture is used to reduce the irreversibility loss. Therefore, the exergy efficiency improvement is clearly more obvious at lower ambient temperatures, which is consistent with the conclusion that the effect of the CO<sub>2</sub>/R32 mixture is more significant in a cold climate region.



**Figure 11.** Comparison of the exergy efficiency with pure CO<sub>2</sub> and CO<sub>2</sub>/R32 mixture refrigerants under a range of ambient temperatures.

#### 4. Case Study

China covers a vast territory, and the climate can be divided, in line with the Chinese standard GB 50178-93 [29], into the following five zones: (I) Severe cold region; (II) Cold region; (III) Hot summer and cold winter region; (IV) Temperate region, and (V) Hot summer and warm winter region. Consideration of the DHW load is mainly determined by the residential behaviors, and one case study in Xi'an city is presented in this section. Detailed information, including ambient temperature as well as the DHW load, is obtained from the literature [30] and shown in Figure 12.

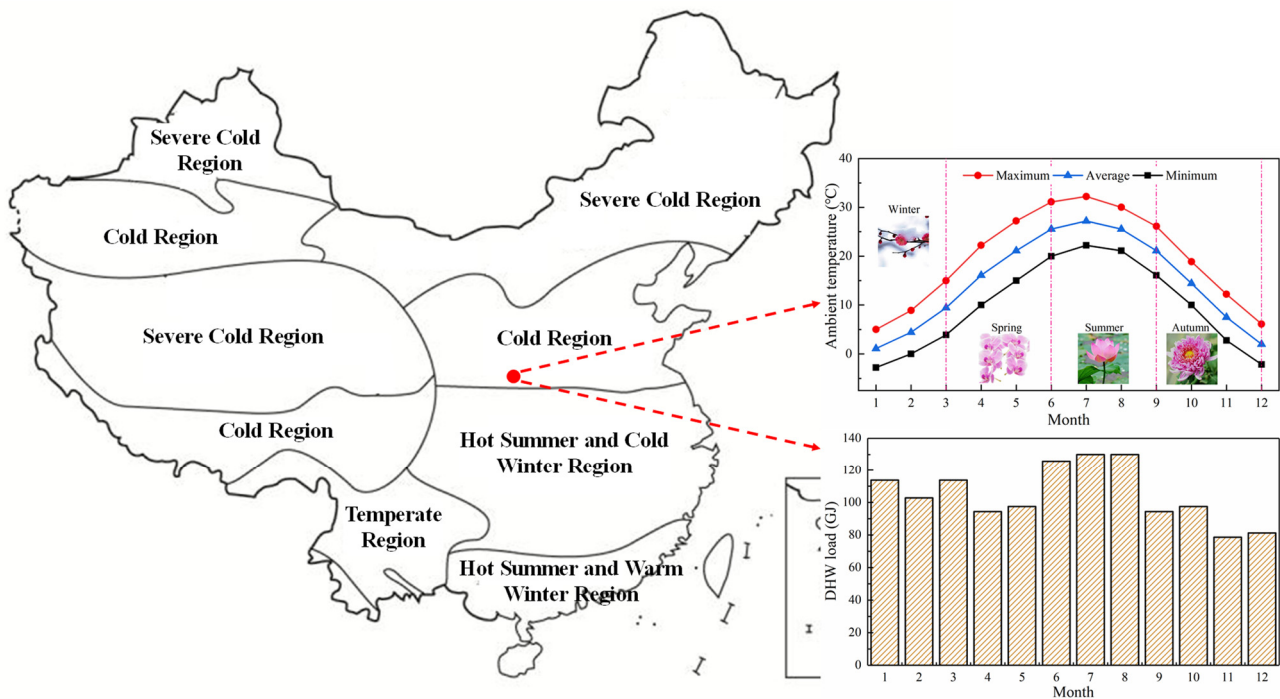


**Figure 12.** Location and detailed information of Xi'an city.

For the air source heat pump, the common tendency of the COP is for it to increase with the higher ambient temperature, regardless of the refrigerant charged into the heat pump system. Figure 13 shows the system COP for each refrigerant cycle in each month related to ambient temperature. As illustrated in Figure 12, the highest and lowest ambient temperatures are seen in July and January, respectively. Compared with the pure CO<sub>2</sub> cycle, the COP improvement is more significant at the higher ambient temperature achieved by the CO<sub>2</sub>/R32 mixture cycle. Specifically, the maximum COP improvement is 7.14% in July, and the minimum improvement is 3.83% in January. Overall, the COP improvement during the year is beneficial for the annual heating performance enhancement, which will be discussed below.

In order to compare the annual heating performance of the same system charged with pure CO<sub>2</sub> and with CO<sub>2</sub>/R32 mixture refrigerants as working fluids, two indicators, annual performance factor and annual exergy efficiency, are selected to show system improvement. For the evaluation of the annual exergy efficiency, the exergy efficiency at each month is first calculated, where  $T_0$  refers to the average ambient temperature of each month. Figure 14 shows the comparison results of the two refrigerant cycles. Compared with the pure CO<sub>2</sub> cycle, which is considered as the baseline system, the annual performance factor and annual exergy efficiency are increased by 5.39% and 3.11%, respectively, with the CO<sub>2</sub>/R32 mixture cycle. It is, therefore, clear that a better heating performance can be obtained with the proposed mixture cycle.

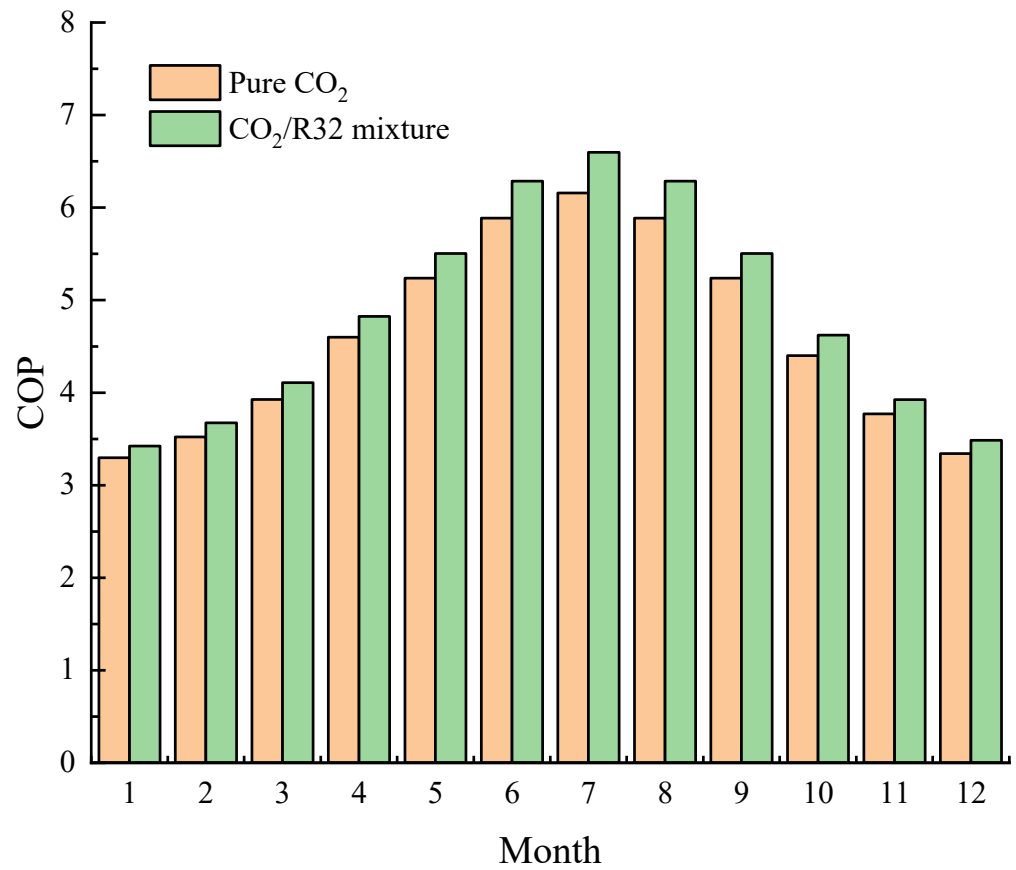


Figure 13. Comparison of the COP with pure CO<sub>2</sub> and CO<sub>2</sub>/R32 mixture refrigerants by month in Xi'an city.

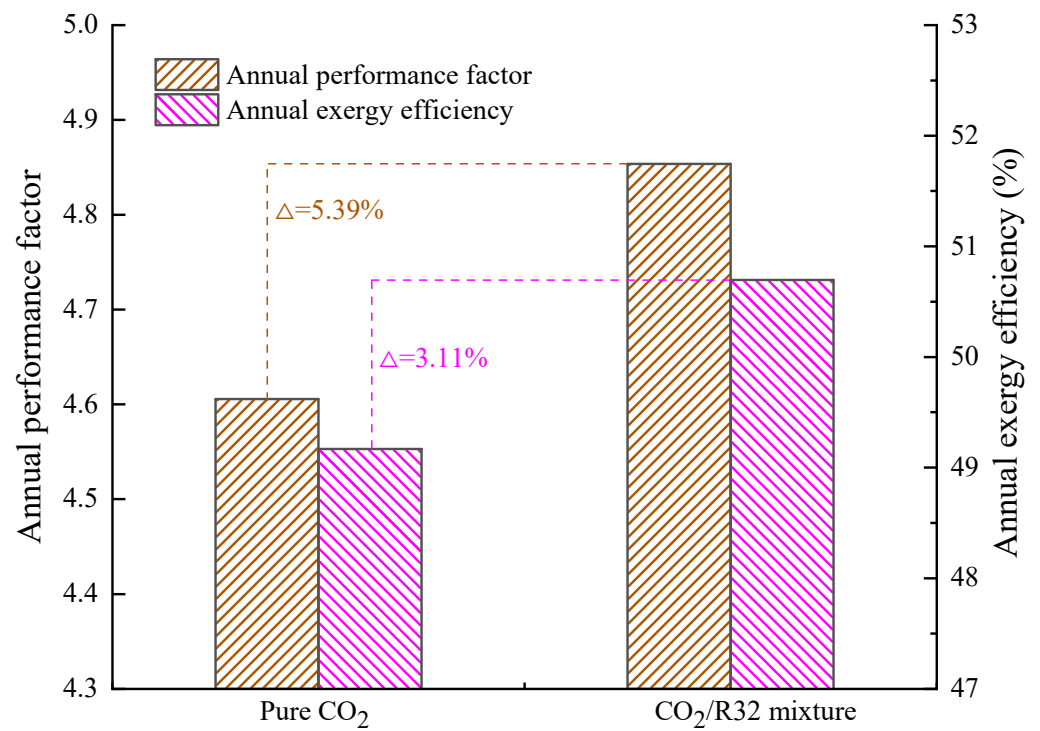


Figure 14. Comparison of the annual performance factor and annual exergy efficiency with pure CO<sub>2</sub> and with CO<sub>2</sub>/R32 mixture refrigerants.

In order to more intuitively reflect the beneficial impact of the CO<sub>2</sub>/R32 mixture refrigerant on the reduction of energy consumption throughout the year, the notion of primary energy consumption (PEC) was adopted. The prevailing coal-fired boiler (CFB) and direct electric heater (DEH) used in China were also chosen.

The PEC can be calculated as:

$$PEC_{TCHP} = E_h ECF_{ele} / (COP \eta_t) \quad (17)$$

$$PEC_{CFB} = E_h ECF_{coal} / (LHV_{coal} \eta_h \eta_t) \quad (18)$$

$$PEC_{DEH} = E_h ECF_{ele} / (\eta_t \eta_h) \quad (19)$$

where the DHW load ( $E_h$ ) has been presented in Figure 12.

The interpretations of the items listed in Equations (17)–(19) are presented in Table 3.

**Table 3.** Items regarding the PEC calculation.

Item	Interpretation	Unit	Coal	Electricity
ECF	energy conversion factor	kgce·kg <sup>-1</sup> ; kgce·(kW·h) <sup>-1</sup>	1	0.4
$\eta_h$	heating efficiency	%	0.75	0.99
$\eta_t$	transmission efficiency	%	0.8	0.92
LHV	lower heating value	kJ kg <sup>-1</sup>	29307	-

Data from [30].

Figure 15 depicts the primary energy consumption of the four heating solutions discussed. Compared with the CO<sub>2</sub>/R32 mixture cycle, an additional 1.64 tce of primary energy consumption is required by the baseline pure CO<sub>2</sub> system, since the calculated primary energy consumption is relevant to the annual performance factor as shown in Figure 14. Based on Equation (17), the higher DHW load will result in a larger primary energy consumption reduction. For the primary energy consumption among the four solutions discussed, DEH presents the maximum at 153.66 tce, and CFB presents the second largest at 71.63 tce. This also indicates that these two prevailing solutions should be replaced with a TCHP for hot water. The PEC of the CO<sub>2</sub>/R32 mixture system can be reduced by 78.93% and 54.80%, respectively, when compared with these two solutions.

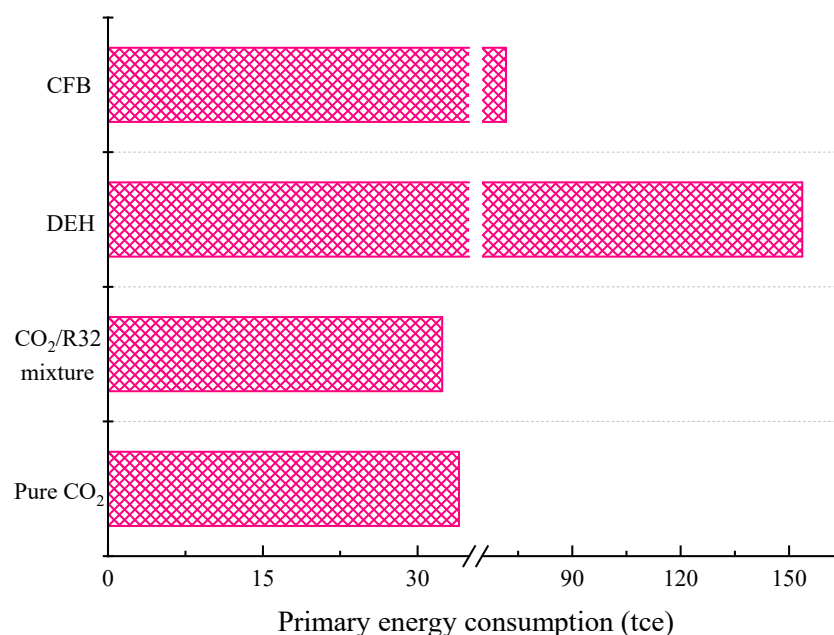


**Figure 15.** Comparison of the primary energy consumption.

## 5. Conclusions

In this study, a CO<sub>2</sub>/R32 mixture refrigerant for use in a transcritical CO<sub>2</sub> heat pump is investigated, and a case study is also presented to show the benefit of the determined optimal CO<sub>2</sub>/R32 concentration. The main conclusions are that:

1. The maximum temperature glide of 14.20 °C and maximum critical pressure of 7.58 MPa can be observed with the R32 mass fractions of 0.6 and 0.2, respectively. The GWP and critical temperature of the CO<sub>2</sub>/R32 mixture are always increased with the larger R32 mass fraction.
2. The COP and exergy efficiency variation show an “M” shape trend, and these two parameters are lower than that of the pure CO<sub>2</sub> cycle if the R32 mass fraction is within the range 0.4–0.6. The optimal pressure reduction is increased and the irreversibility of the EEV is reduced from 0.031 to 0.009 kW·kW<sup>-1</sup> in relation to the increased R32 mass fraction.
3. With regard to flammability and efficiency, the optimal concentration of the CO<sub>2</sub>/R32 mixture is determined as 0.9/0.1. Over an ambient temperature range of –15 to 25 °C, the COP and exergy efficiency improvements are more notable in a cold climate, since the total irreversibility reduction is more remarkable.
4. In the selected typical city, the case study results show that the annual performance factor and annual exergy efficiency can be increased by 5.39% and 3.11%, respectively, with the CO<sub>2</sub>/R32 mixture cycle, leading to a 1.64 tce reduction in primary energy consumption.

**Author Contributions:** Conceptualization, Y.W. and Y.S.; methodology, Y.W.; software, Y.W.; validation, Y.W. and Y.H.; formal analysis, Y.W. and Y.H.; investigation, Y.W.; resources, Y.S. and F.C.; data curation, Y.W.; writing—original draft preparation, Y.W.; writing—review and editing, all authors; visualization, Y.W. and Y.H.; supervision, F.C.; project administration, F.C.; funding acquisition, F.C. All authors have read and agreed to the published version of the manuscript.

**Funding:** This research was funded by the National Natural Science Foundation of China (No. 51976153), National Science and Technology Major Project (2017-III-0010-0036), and Foundation for Innovative Research Groups of the National Natural Science Foundation of China (No.51721004).

**Conflicts of Interest:** The authors declare no conflict of interest.

## Nomenclature

### Latin symbols

$E_h$	domestic hot water load, kJ
ECF	energy conversion factor, kgce·kg <sup>-1</sup> , kgce·(kW·h) <sup>-1</sup>
$ir$	irreversibility per unit heating capacity, kW·kW <sup>-1</sup>
$I_k$	irreversibility of each component, kW
LHV	lower heating value, kJ·kg <sup>-1</sup>
$m$	mass flow rate, kg·s <sup>-1</sup>
$P$	pressure, MPa
$Q$	heating capacity, kW
$T$	temperature, °C
$W$	power consumption, kW

### Greek symbols

$\eta$	efficiency, %
--------	---------------

### Abbreviations

ASHP	air source heat pump
CFB	coal-fired boiler
COP	coefficient of performance
DEH	direct electric heater
GWP	global warming potential
IHX	internal heat exchanger
ODP	ozone depletion potential
PEC	primary energy consumption
TCHP	transcritical CO <sub>2</sub> heat pump

### Subscripts

0	ambient (dead state)
a	air
c	cooling
coal	coal
Comp	compressor
d	discharge
e	electrical efficiency
ele	electricity
Evap	evaporator
GC	gas cooler
h	heating
i	inlet
is	isentropic efficiency
m	mechanical efficiency
Mix	mixture refrigerant
o	outlet
r	refrigerant
t	transmission
Tot	total
w	water

### References

- Chang, C.; Zhu, N.; Yang, K.; Yang, F. Data and analytics for heating energy consumption of residential buildings: The case of a severe cold climate region of China. *Energy Build.* **2018**, *172*, 104–115. [[CrossRef](#)]
- Wang, Y.K.; Ye, Z.L.; Song, Y.L.; Yin, X.; Cao, F. Experimental investigation on the hot gas bypass defrosting in air source transcritical CO<sub>2</sub> heat pump water heater. *Appl. Therm. Eng.* **2020**, *178*, 115571. [[CrossRef](#)]
- Wang, F.; Zhao, R.; Xu, W.; Huang, D.; Qu, Z. A Heater-Assisted Air Source Heat Pump Air Conditioner to Improve Thermal Comfort with Frost-Retarded Heating and Heat-Uninterrupted Defrosting. *Energies* **2021**, *14*, 2646. [[CrossRef](#)]
- Xu, Y.; Mao, C.; Huang, Y.; Shen, X.; Xu, X.; Chen, G. Performance evaluation and multi-objective optimization of a low-temperature CO<sub>2</sub> heat pump water heater based on artificial neural network and new economic analysis. *Energy* **2021**, *216*, 119232. [[CrossRef](#)]
- Kim, M.S.; Kang, D.H.; Kim, M.S.; Kim, M. Investigation on the optimal control of gas cooler pressure for a CO<sub>2</sub> refrigeration system with an internal heat exchanger. *Int. J. Refrig.* **2017**, *77*, 48–59. [[CrossRef](#)]
- Taslimi Taleghani, S.; Sorin, M.; Poncet, S.; Nesreddine, H. Performance investigation of a two-phase transcritical CO<sub>2</sub> ejector heat pump system. *Energy Convers. Manag.* **2019**, *185*, 442–454. [[CrossRef](#)]
- Yang, J.L.; Ma, Y.T.; Li, M.X.; Guan, H.Q. Exergy analysis of transcritical carbon dioxide refrigeration cycle with an expander. *Energy* **2005**, *30*, 1162–1175. [[CrossRef](#)]
- Dai, B.M.; Qi, H.F.; Liu, S.C.; Ma, M.Y.; Zhong, Z.F.; Li, H.L.; Song, M.J.; Sun, Z.L. Evaluation of transcritical CO<sub>2</sub> heat pump system integrated with mechanical subcooling by utilizing energy, exergy and economic methodologies for residential heating. *Energy Convers. Manag.* **2019**, *192*, 202–220. [[CrossRef](#)]
- Elbel, S.; Hrnjak, P. Flash gas bypass for improving the performance of transcritical R744 systems that use microchannel evaporators. *Int. J. Refrig.* **2004**, *27*, 724–735. [[CrossRef](#)]
- Chesi, A.; Esposito, F.; Ferrara, G.; Ferrari, L. Experimental analysis of R744 parallel compression cycle. *Appl. Eng.* **2014**, *135*, 274–285. [[CrossRef](#)]

11. Zhang, Z.; Wang, H.; Tian, L.; Huang, C. Thermodynamic analysis of double-compression flash intercooling transcritical CO<sub>2</sub> refrigeration cycle. *J. Supercrit. Fluids* **2016**, *109*, 100–108. [[CrossRef](#)]
12. De Antonellis, S.; Joppolo, C.M.; Liberati, P.; Milani, S.; Romano, F. Modeling and experimental study of an indirect evaporative cooler. *Energy Build.* **2017**, *142*, 147–157. [[CrossRef](#)]
13. Yu, B.; Yang, J.; Wang, D.; Shi, J.; Chen, J. An updated review of recent advances on modified technologies in transcritical CO<sub>2</sub> refrigeration cycle. *Energy* **2019**, *189*, 116147. [[CrossRef](#)]
14. Wang, D.; Liu, Y.; Kou, Z.; Yao, L.; Lu, Y.; Tao, L.; Xia, P. Energy and exergy analysis of an air-source heat pump water heater system using CO<sub>2</sub>/R170 mixture as an azeotropy refrigerant for sustainable development. *Int. J. Refrig.* **2019**, *106*, 628–638. [[CrossRef](#)]
15. de Paula, C.H.; Duarte, W.M.; Rocha, T.T.M.; de Oliveira, R.N.; Mendes, R.d.P.; Maia, A.A.T. Thermo-economic and environmental analysis of a small capacity vapor compression refrigeration system using R290, R1234yf, and R600a. *Int. J. Refrig.* **2020**, *118*, 250–260. [[CrossRef](#)]
16. Niu, B.; Zhang, Y. Experimental study of the refrigeration cycle performance for the R744/R290 mixtures. *Int. J. Refrig.* **2007**, *30*, 37–42. [[CrossRef](#)]
17. Zhang, X.P.; Wang, F.; Fan, X.W.; Wei, X.L.; Wang, F.K. Determination of the optimum heat rejection pressure in transcritical cycles working with R744/R290 mixture. *Appl. Therm. Eng.* **2013**, *54*, 176–184. [[CrossRef](#)]
18. Ju, F.; Fan, X.; Chen, Y.; Ouyang, H.; Kuang, A.; Ma, S.; Wang, F. Experiment and simulation study on performances of heat pump water heater using blend of R744/R290. *Energy Build.* **2018**, *169*, 148–156. [[CrossRef](#)]
19. Ju, F.; Fan, X.; Chen, Y.; Wang, T.; Tang, X.; Kuang, A.; Ma, S. Experimental investigation on a heat pump water heater using R744/R290 mixture for domestic hot water. *Int. J. Therm. Sci.* **2018**, *132*, 1–13. [[CrossRef](#)]
20. Wang, D.; Lu, Y.; Tao, L. Thermodynamic analysis of CO<sub>2</sub> blends with R41 as an azeotropy refrigerant applied in small refrigerated cabinet and heat pump water heater. *Appl. Therm. Eng.* **2017**, *125*, 1490–1500. [[CrossRef](#)]
21. Dai, B.M.; Dang, C.B.; Li, M.X.; Tian, H.; Ma, Y.T. Thermodynamic performance assessment of carbon dioxide blends with low-global warming potential (GWP) working fluids for a heat pump water heater. *Int. J. Refrig.* **2015**, *56*, 1–14. [[CrossRef](#)]
22. Yu, B.; Yang, J.; Wang, D.; Shi, J.; Guo, Z.; Chen, J. Experimental energetic analysis of CO<sub>2</sub>/R41 blends in automobile air-conditioning and heat pump systems. *Appl. Eng.* **2019**, *239*, 1142–1153. [[CrossRef](#)]
23. Sun, Z.; Cui, Q.; Wang, Q.; Ning, J.; Guo, J.; Dai, B.; Liu, Y.; Xu, Y. Experimental study on CO<sub>2</sub>/R32 blends in a water-to-water heat pump system. *Appl. Therm. Eng.* **2019**, *162*, 114303. [[CrossRef](#)]
24. Lemmon, E.W.; Huber, M.L.; McLinden, M.O. *NIST Standard Reference Database 23, Reference Fluid Thermodynamic and Transport Properties (REFPROP), Version 9.1*; National Institute of Standards and Technology: Gaithersburg, MD, USA, 2013.
25. GB/T21362-2008. Heat Pump Water Heater for Commercial & Industrial and Similar Application. General Administration of Quality Supervision, Inspection and Quarantine of the People's Republic of China. In *Standardization Administration of the People's Republic of China*; General Administration of Quality Supervision, Inspection and Quarantine of the People's Republic of China: Beijing, China, 2008; Volume 1.
26. Brown, J.S.; Zilio, C.; Akasaka, R.; Higashi, Y. Low-GWP refrigerants. *Sci. Technol. Built Environ.* **2016**, *22*, 1075–1076. [[CrossRef](#)]
27. Heberle, F.; Preißinger, M.; Brüggemann, D. Zeotropic mixtures as working fluids in Organic Rankine Cycles for low-enthalpy geothermal resources. *Renew. Energy* **2012**, *37*, 364–370. [[CrossRef](#)]
28. Zabetakis, M.G. *Flammability Characteristics of Combustible Gases and Vapors*; Bureau of Mines: Washington, DC, USA, 1965.
29. GB/T50178-93. Standard of climatic regionalization for architecture. In *Standardization Administration of the People's Republic of China*; State Bureau of Technical Supervision Ministry of Construction of the People's Republic of China: Beijing, China, 1994; Volume 1.
30. Wang, Y.K.; Ye, Z.L.; Song, Y.L.; Yin, X.; Cao, F. Energy, economic and environmental assessment of transcritical carbon dioxide heat pump water heater in a typical Chinese city considering the defrosting. *Energy Convers. Manag.* **2021**, *233*, 113920. [[CrossRef](#)]